JOURNAL OF THERMOPHYSICS AND HEAT TRANSFER
Vol. 24, No. 1, January–March 2010

Spray Cooling Heat Flux Performance Using POCO HTC Foam

Eric A. Silk*
NASA Goddard Space Flight Center, Greenbelt, Maryland 20771
and
Philip Bracken†
Rensselaer Polytechnic Institute, Troy, New York, 12180

DOI: 10.2514/1.44089

Previous studies have shown that spray cooling heat flux enhancement may be attained using enhanced surfaces. Most enhanced surface spray cooling studies have been performed using either extended or embedded surface structures. The present study investigates the effect of POCO HTC foam on spray cooling heat flux. The copper blocks used in the heat flux performance study had a cross-sectional area of 2.0 cm^2. The POCO HTC foam pieces were attached to the copper blocks using two different bonding techniques. These were S-Bond® soldering and high thermal conductivity epoxy as the thermal interface material. Measurements were also obtained on a heater block with a flat surface for purposes of baseline comparison. A 2 × 2 nozzle array was used with PF-5060 as the working fluid. Thermal performance data was obtained under nominally degassed conditions (chamber pressure of 41.4 kPa). Results show that the highest heat flux attained was 133 W/cm^2 using the graphite POCO HTC foam with a nozzle-to-foam distance of 17 mm.

Nomenclature

A	=	area
c_p	=	specific heat, J/kg°C
h_{fg}	=	enthalpy of vaporization, kJ/kg
k	=	thermal conductivity, $W/m \cdot K$
P	=	pressure
ρ_l	=	liquid density, kg/m^3
$\dot{q}''$	=	heat flux per unit area
R	=	thermal resistance, $(T_{surf} - T_{liq})/(\dot{q}''_{CHF} A_{surf})$
T	=	temperature
$\dot{V}$	=	volume flow rate, ml/ min
$\dot{V}''$	=	volumetric flux, $m^3/m^2 \cdot s$
x	=	distance from heater surface within heater, m
ΔT_{sup}	=	$T_{surf} - T_{sat}$, °C
δ_k	=	error in conductivity
δ_x	=	error in thermocouple location
$\delta_{\Delta T}$	=	error in thermocouple temperature difference
$\delta\dot{q}''$	=	error in heat flux
$\eta_{2\text{-}\phi}$	=	$\dot{q}''/\rho\dot{V}''[c_{p,l}(T_{sat} - T_l) + h_{fg}]$

Subscripts

flat	=	flat surface
k	=	conductivity
l	=	liquid
CHF	=	critical heat flux
max	=	maximum
r	=	radial direction
sat	=	saturation conditions
surf	=	surface
T	=	temperature
x	=	thermocouple distance
Θ	=	theta direction
Z	=	z direction
1-ϕ	=	single phase
2-ϕ	=	multiphase

Received 1 March 2009; revision received 10 June 2009; accepted for publication 9 July 2009.

*Associate Branch Head, Cryogenics and Fluids Branch, Building 7, Room 109; Eric.A.Silk@nasa.gov.

†Summer Research Assistant, Department of Mechanical, Aerospace, and Nuclear Engineering, Jonsson Engineering Center, Room 2049, 110 8th Street.

I. Introduction

SPRAY cooling is a multiphase heat transfer process that has gained much attention in recent years as a thermal solution to high-heat-flux temperature control problems in the electronics, aerospace, and naval industries. A review of spray cooling literature shows that there have been several studies conducted to gain a better understanding of the phenomena associated with the spray cooling heat transfer process. Previous studies performed have parametrically examined the effect of secondary gas atomizers versus pressure atomizers [1,2], mass flux of ejected fluid [3,4], spray velocity [5,6], droplet impact velocity [5,7,8], surface roughness [1,6,9,10], ejected fluid temperature, chamber environmental conditions, and spray footprint optimization on the effective heat flux across the heater surface [11]. Other topics investigated include the effect of surfactant addition [12,13] and secondary nucleation [1,14,15].

Previous studies that have examined enhanced surfaces have primarily focused on surface enhancements such as surface roughness [1,10] and microstructured surfaces [16]. However, as interest in spray cooling grows, enhanced surface spray cooling investigations emphasizing structure enhancements beyond the surface roughness level are also increasing in number. In the study by Silk et al. [17], the effects of enhanced surface structures beyond the surface roughness range on spray cooling heat transfer were investigated. The surface enhancements consisted of cubic pin fins, pyramids, and straight fins machined on the top surface of copper heater blocks with a 2.0 cm^2 cross-sectional area. Measurements were also obtained on a flat surface heater for data comparison. PF-5060 under nominally degassed conditions (chamber pressure of 41.4 kPa) was used as the working fluid. The spray volumetric flux (0.016 $m^3/m^2 \cdot s$) and nozzle-to-heater distance (≈17 mm) were held constant throughout each test. The spray temperature was 20.5°C. The study showed that the straight fins had the largest heat flux enhancement relative to the flat surface, followed by the cubic pin fins and the pyramid surface. Each surface had an increase in evaporation efficiency at critical heat flux (CHF) compared with the flat surface. The authors determined that the straight finned surface had the most efficient use of area added for additional heat transfer relative to the flat surface. They also determined that heat flux enhancement observed with the use of

enhanced surfaces is a function of surface area added and liquid management on the heater.

Coursey et al. [18] investigated spray cooling of high-aspect-ratio open microchannels with a full cone nozzle. The study included five heat sinks each with a projected surface area of 1.41×1.41 cm^2, a channel width of 360 μm, and a fin width of 500 μm. Fin heights tested ranged between 0.25 and 5.0 mm. A flat surface with the same projected surface area as the enhanced surfaces was also tested for data comparison purposes. PF-5060 at $T_{sat} = 30$°C was used as the working fluid. Studies were performed with nozzle pressures in the range of 137.8 $\leftrightarrow$ 413.4 kPa. The study showed that heat flux performance for each of the enhanced surfaces improved relative to the flat surface's performance. The authors determined that longer fins outperform shorter ones in the single phase regime, and that the addition of fins resulted in multiphase effects at lower wall temperatures compared with the flat surface. The studies also showed that the use of enhanced surfaces increased the phase change efficiency in comparison to the flat surface case. Fin heights between 1.0 and 3.0 mm provided optimum heat flux performance for the test conditions studied.

There have been several studies performed using porous foam and microporous surfaces as a heat flux enhancement technique for forced convection [19–21], thermosyphons [22], pool boiling [23–25], and thermal energy storage [26] applications. Jamin and Mohamad [20] performed a forced convection study to quantify heat transfer enhancement for POCO HTC foam (manufactured by Poco Graphite, Inc.) in crossflow. Measurements were taken for the heat transfer rate and pressure drop for a heated vertical pipe with and without the porous foam. The copper pipe had an o.d. of 15.875 mm and a length of 152.2 mm. These dimensions were constant for all the cases studied. Tests were performed over a range of velocities ($\approx$8 $\leftrightarrow$ 45 m/s) using air as the working fluid. The studies showed that the POCO HTC foam enhanced heat transfer by factors ranging from 1.3 to 3.05 relative to the bare copper surface's heat transfer performance. However, use of the foam resulted in increased pressure drop across the test section. The authors determined that this was due to the low permeability of the foam, which created a large resistance to fluid flow inside the porous media.

Coursey et al. [22] investigated the thermal performance of a graphite foam thermosyphon evaporator. The graphite foam used in their study was Poco Foam (manufactured by Poco Graphite, Inc.). Multiple foam samples with variations in height, width, and density were bonded to copper heaters each with a cross-sectional area of 1.0 cm^2. Evaporator performance was examined using FC-72 and FC-87 as working fluids. The effects of liquid fill level and condenser temperature as well as foam height, width, and density were studied. The study results showed that the heat transfer performance of the two working fluids was similar. However, the liquid fill level, condenser temperature, geometry, and density of the graphite foam had a significant effect upon thermal performance. The authors determined that the boiling process was surface-tension dominated. The highest heat transfer attained in this study was 149 W.

In the study by Parker and El-Genk [24], orientation effects upon nucleate boiling were investigated for a porous graphite and a smooth copper surface. Inclination angles for the orientations investigated ranged from a 0 deg (heater normal facing upward) to 180 deg inclination (heater normal facing downward). The projected area for heat exchange was 10×10 mm^2 for both heaters. The porous graphite and flat copper surface were attached to the heating elements on their test section using high-thermal-conductivity epoxy. Degassed FC-72 was used as the working fluid. Nucleate boiling heat flux, the nucleate boiling heat transfer coefficient, and CHF were reported and compared. The study showed that the highest CHFs were attained for both the porous and the flat surfaces in the upward-facing orientation (i.e., 0 deg orientation) and had values of 30 and 18 W/cm^2, respectively. The study also showed that the porous graphite surface had consistently higher CHF values than the flat copper surface for all orientations tested.

In the study by Silk and Dick [27], the effects of porous graphite Poco Foam (as an enhanced surface) on spray cooling heat transfer were investigated. The Poco Foam was machined into the shape of a cylinder with a height of 5.9 mm and a diameter of 16 mm (i.e., top and bottom surfaces' cross-sectional area was 2.0 cm^2). The foam was attached to a flat surface on the top of a copper heater block using high-thermal-conductivity epoxy (Stycast 2850 FT/Catalyst 11) as the thermal interface material (TIM). PF-5060 under nominally degassed conditions (chamber pressure of 41.4 kPa) was used as the working fluid. The spray volumetric flux was varied (0.01 $\leftrightarrow$ 0.016 m^3/m$^2 \cdot$ s), whereas the nozzle-to-copper heater surface distance ($\approx$17 mm) and spray temperature (20.5°C) were held constant throughout each test. The study showed that extensive superheating occurred at the copper/foam bond line for the Poco Foam cases. The Poco Foam surface provided heat flux enhancement relative to the flat surface for each volumetric flux case only after reaching extensive superheat levels. The extensive superheat levels attained with the Poco Foam were primarily attributed to the foam's thermal resistance to the heat flow path.

Previous enhanced surface spray cooling studies [17,18,28] have shown that spray cooling of enhanced surfaces (e.g., extended fins and porous tunnels) results in a corresponding heat flux enhancement. In addition, the Poco Foam spray cooling study by Silk and Dick [27] showed that heat transfer enhancement using graphite foam is possible when performing spray cooling. The present investigation extends the graphite foam spray cooling work of Silk and Dick [27] by studying spray cooling heat flux performance using POCO HTC foam as a surface enhancement with both epoxy and S-Bond soldering as bonding techniques for foam attachment to the copper block. Heat flux as a function of volume flow rate is reported for the POCO HTC foam samples. Heat flux data attained using POCO HTC foam as a surface enhancement are also compared with those of a flat copper surface with the same projected heater surface area. It was observed that the POCO HTC foam surface provided a heat flux enhancement relative to the flat surface data. Also, superheat levels at the copper/foam interface were noticeably less when using the S-Bond soldering technique than those observed when using high-thermal-conductivity epoxy as the TIM.

II. Experimental Apparatus and Data Reduction

A. Test Setup and Procedure

The experiments were conducted using a closed fluid loop system. The test rig (schematic shown in Fig. 1) consisted of an environmental test chamber, liquid pump, flow meter, microfilter, and condenser. The chamber temperature and pressure were measured via a T-type thermocouple (T) and a pressure sensor. Temperature and pressure sensors were also placed in the liquid line upstream of the nozzle for fluid and supply line temperature and pressure measurement. Heat was supplied to the test article using a 500 W cartridge heater. The test article was placed interior to the chamber and was separated from the excess liquid by an enclosure consisting of a polycarbonate housing and an alumina bisque ceramic top flange

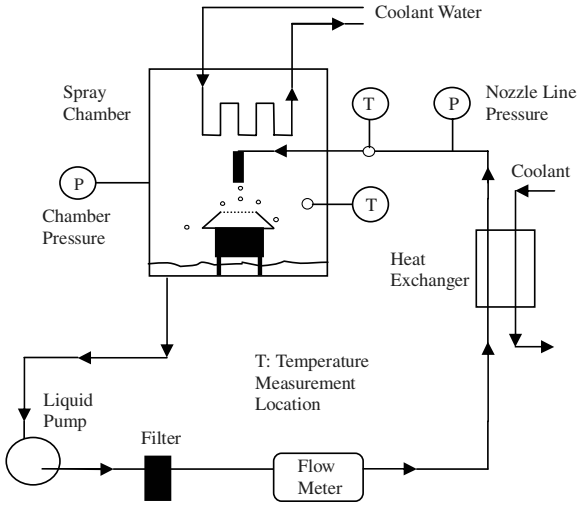

Fig. 1 Spray cooling test rig configuration.

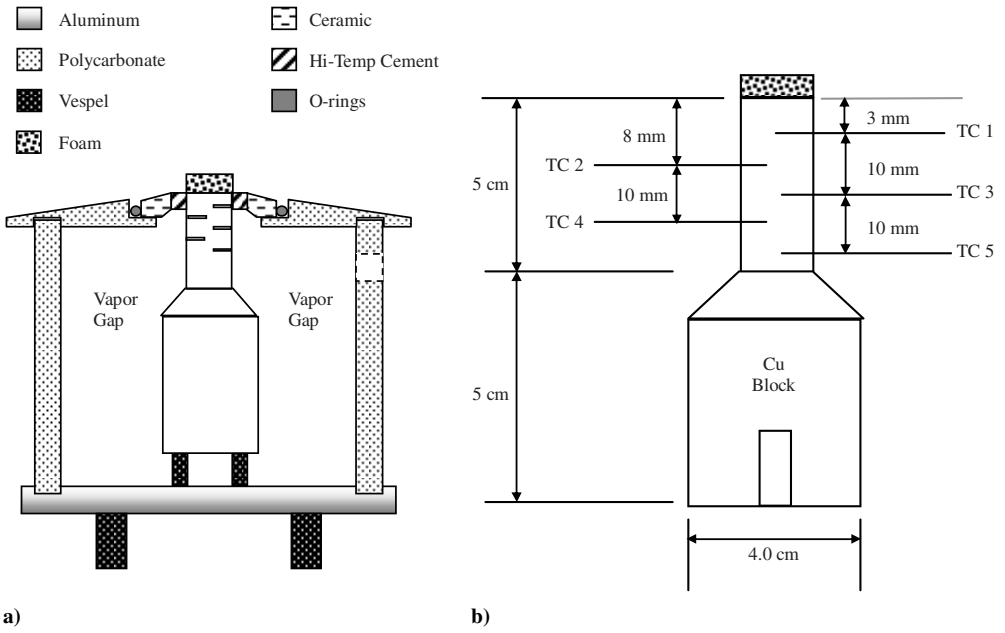

Fig. 2 Copper block schematic: a) housing, and b) TC locations.

(Fig. 2a). The upper section of the copper block was epoxied to the ceramic flange. Temperature measurements in the copper blocks were taken via five T-type thermocouples mounted in the upper section of each block (shown in Fig. 2b). Assuming steady-state one-dimensional conduction through the upper portion of the block, the heat flux was calculated using Fourier's law. The heat flux was determined as the average value from multiple pairs of thermocouples (TC1–5). The surface temperature was determined via linear extrapolation using TC1 and 2. Before each test, the spray chamber and fluid loop were charged with PF-5060 and a vacuum was repeatedly applied to the chamber until a pressure of 41.4 kPa was reached. The chamber was allowed to attain equilibrium before initiating heat flux performance testing. Test conditions are shown in Table 1.

B. Spray Nozzle Array

A Parker Hannifin spray nozzle consisting of a 2 × 2 spray cone array was used for each of the tests (a close-up of the comprehensive spray is shown in Fig. 3). Based on the nozzle-to-heater surface distance used in previous analogous flat surface tests (17 mm) with the same heater surface area and spray configuration, the volumetric flux at the center of the heater surface is twice as much as the average for the entire heater surface. Toward the perimeter of the heater surface, the volume flux reduces to as low as 40% of the average area value. Thus, the spray can be considered a nonuniform center-biased spray. For a detailed explanation of the volume flux experiment performed previously, please see Silk et al. [17].

C. POCO HTC Foam Attachment

The porous graphite foam used in the present study was POCO HTC foam, which is manufactured by Poco Graphite, Inc. The

Table 1 Test case conditions

Spray cooling parameters	
Parameters	Values
P_{sat}, kPa	41.4
T_{sat}, °C	31
T_l, °C	20.5
h_{fg}, kJ/kg	92
Gas content, ppm	428

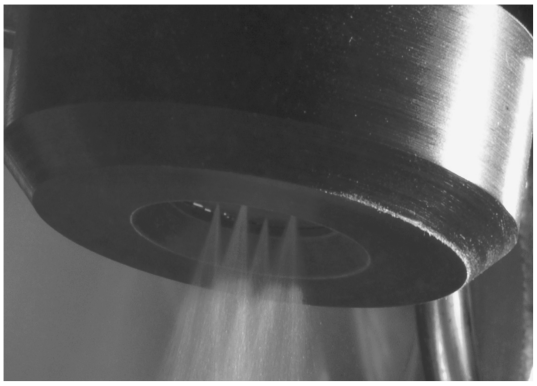

Fig. 3 Spray manifold close-up of 2 × 2 nozzle array.

POCO HTC foam was machined into the shape of a cylinder with a height of 5.9 mm and an approximate diameter of 16 mm (size scale photo shown in Fig. 4). This gave the top and bottom sides of the foam cylinder a cross-sectional area of 2.0 cm^2. Table 2 lists the properties of the POCO HTC foam. As mentioned earlier, two different bonding techniques were used in the present study (i.e., high thermal conductivity epoxy and S-Bond soldering). For the epoxy bonding case (i.e., HTC epoxy TIM case), the top surface of the copper block was slightly roughened (using Scotch-Brite™)

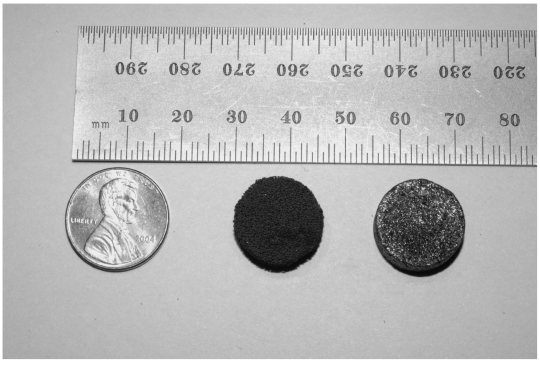

Fig. 4 Photos of foam structures.

Table 2 Summary of foam properties

Property	POCO HTC foam
Average pore diameter	$\approx$350 μm
Open porosity	95%
Total porosity	61%
Density (ρ)	0.9 g/cm^3
Planar conductivity ($k_r = k_\theta$)	70 W/m $\cdot$ K
Out-of-plane conductivity (k_z)	245 W/m $\cdot$ K

before attachment of the foam for better adherence of the bonding material. The porous POCO HTC foam was then bonded to the top surface of the copper block using a thin layer ($\leq$ 0.1 mm) of high-thermal-conductivity epoxy (Stycast 2850 FT/Catalyst 11 by Emerson and Cuming, Inc.). The thermal conductivity of the epoxy was approximately 1.3 W/m $\cdot$ K. The copper/foam TIM was then cured at 120°C for 1 h before testing. For the S-Bond soldering case the bonding procedure was performed by S-Bond Technologies. The procedure entailed treating the mating side of the foam with an S-Bond powder composition (S-Bond alloy 220). This was then fused to the foam at temperatures in excess of 700°C. Afterward, S-Bond alloy (in paste form) was spread onto the base material (i.e., the top of the copper heater block). Both the copper heater block and the metallized POCO HTC foam test piece were then heated again. Upon reaching the desired bonding temperature, the metallized foam and the S-Bond-treated copper surface were pressed together and allowed to cool back down to room temperature.

D. Nozzle-to-Heater Surface Distance

All of the flat surface flow rate tests were performed using a constant nozzle-to-heater surface distance of 17 mm. For the HTC epoxy TIM case, the nozzle height was held constant (with respect to the flat surface case), thus making the nozzle height relative to the copper/foam interface 17 mm and the nozzle-to-foam distance approximately 11.1 mm. The spray cooling studies performed using the POCO HTC foam attached to the copper block via S-Bond soldering used two different nozzle heights relative to the copper/foam interface (17 and 23 mm). Similar to the HTC epoxy TIM case, the study for the nozzle height of 17 mm (relative to the copper/foam interface) had a distance of 11.1 mm between the POCO HTC foam's top surface and the spray nozzle. By making the nozzle height constant, an underspray condition on the foam's top surface was created. However, in the larger nozzle height case ($\approx$23.0 mm) the distance between the spray nozzle and the top of the foam (i.e., the nozzle-to-foam distance) is actually the same as the nozzle-to-heater surface distance in the flat surface case. By preserving the distance of 17.0 mm between the spray nozzle and the impingement surface, liquid spray coverage of the foam's top surface is optimized. Henceforth, the study case using the nozzle height of 17.0 mm is referred to as the HTC S-Bond short case. The study case with the nozzle height of approximately 23.0 mm is referred to as the HTC S-Bond optimum case.

E. Measurement Uncertainty

The primary quantity of interest for these experiments is the heat flux. The heat flux calculation has three contributions to the uncertainty: the conductivity, the thermocouple locations, and the error in the temperature measured. The conductivity value used was 389 W/m $\cdot$ K with an estimated error of 1%. The error in the thermocouple temperature measurements was estimated as $\pm$0.5°C. The error in the thermocouple location was determined to be $\pm$0.56 mm. Equation (1) was used to calculate the error for the heat flux values reported. The maximum uncertainty in the heat flux was determined to be 5.8% at 133 W/cm^2. Calculations indicated that heat losses within the upper neck of the copper block were less than 1% of the total heat input at CHF for the flat surface case. Pressure values had an uncertainty of $\pm$3 kPa. Flow meter measurements had an error of $\pm$1 ml/ min.

$$\delta\dot{q}'' = \pm\sqrt{\left(\frac{\partial\dot{q}''}{\partial x}\delta_x\right)^2 + \left(\frac{\partial\dot{q}''}{\partial k}\delta_k\right)^2 + \left(\frac{\partial\dot{q}''}{\partial(\Delta T)}\delta_{\Delta T}\right)^2} \quad (1)$$

III. Results and Discussion

The heat flux performance as a function of superheat and flow rate for the flat surface, HTC epoxy TIM, HTC S-Bond short, and HTC S-Bond optimum cases are shown in Figs. 5a–5e. The calculated heat flux is based on the projected heater surface area (2.0 cm^2) for each of the cases. Volume flow rates tested ranged from 120 to 200 ml/ min (a volumetric flux of 0.010–0.016 m^3/m^2 $\cdot$ s). The superheat was defined as the difference between the copper surface temperature and the working fluid saturation temperature. For the POCO HTC foam cases, the copper surface temperature was taken at the copper/foam interface. In each of the flat surface study cases, tests were performed up to CHF. In the HTC epoxy TIM case, tests were performed up to a copper surface temperature (at the copper/foam interface) of approximately 115°C for the lower volume flow rates (i.e., 120–180 ml/ min) due to concerns regarding possible failure of the copper/foam TIM at elevated temperatures, as well as concerns regarding possible dissociation of fluorine gas from the working fluid [29]. Heat flux testing at the largest flow rate (200 ml/ min) was performed up to CHF (shown in Fig. 5e). Unlike the HTC epoxy TIM case, the HTC S-Bond short and optimum tests were performed up through CHF at each flow rate.

In each of the Fig. 5 plots the spray cooling curves are clustered together in the sensible heating portion of the curves ($\Delta T_{sup} \leq 0$°C) with little variation in heat flux performance as a function of the case tested. At each volume flow rate tested the heat transfer variation for each case is linear for $\Delta T_{sup} \leq 11$°C. This is indicative of single-phase convection. At a flow rate of 120 ml/ min, the heat flux curves for each of the cases overlay one another up through $\Delta T_{sup} \approx 11$°C. However, as the flow rate increases from 120 to 200 ml/ min, the flat, HTC S-Bond short, and HTC S-Bond optimum curves all separate from the HTC epoxy TIM case's curves and have higher heat flux performance for 5°C $\leq \Delta T_{sup} <$ 11°C. At each of the flow rates tested, multiphase effects for the flat, HTC S-Bond short, and HTC S-Bond optimum cases become pronounced (denoted by an increase in slope of the heat flux curves) at 11°C $\leq \Delta T_{sup} <$ 15°C. The increase in slope implies that an increase in the convection coefficient has occurred. For the HTC epoxy TIM case tests, the onset of pronounced multiphase effects is observed within the same superheat (11°C $\leq \Delta T_{sup} <$ 15°C) range for flow rates spanning 120–160 ml/ min. However, at flow rates of 180 and 200 ml/ min, the increase in slope is delayed until reaching superheats of 23 and 32°C, respectively. After the onset of pronounced multiphase effects, the heat flux to copper/foam interface superheat relationship remains linear for the HTC epoxy TIM, HTC S-Bond short, and HTC S-Bond optimum cases up to superheat values of 40, 24, and 30°C, respectively. In addition, the HTC S-Bond short and optimum heat flux curves show good agreement for each flow rate at superheat levels upward of $\Delta T_{sup} \approx 24$°C. At $\Delta T_{sup} >$ 24°C, the heat flux curves for these cases separate (with the S-Bond optimum case having higher heat flux) in the approach to CHF. For the HTC epoxy TIM case, the heat flux to copper surface superheat relationship remains fairly constant for all $\Delta T_{sup} >$ 40°C up through CHF at flow rates ranging from 120 to 180 ml/ min. For the 200 ml/ min case, the heat flux undergoes a slight decrease in slope (and convection coefficient) before reaching CHF. The slope of the heat flux curve for the HTC S-Bond short case is linear for $\Delta T_{sup} >$ 24°C up through CHF at each flow rate. For the HTC S-Bond optimum case, the heat flux to superheat relationship remains constant for ΔT_{sup} values spanning 30°C up through CHF at flow rates of 120 and 140 ml/ min. However, similar to the HTC epoxy TIM case, a slight decrease in slope was observed before reaching CHF for the flow rates spanning 160–200 ml/ min. The flat surface's overall heat transfer performance approximated to that of the HTC S-Bond optimum case for $\Delta T_{sup} >$ 11°C up through CHF as the flow rate increased from 120 to 200 ml/ min.

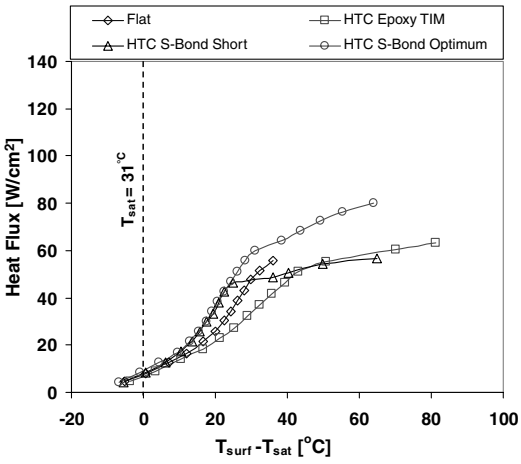

a) Liquid flow rate of 120 ml/min

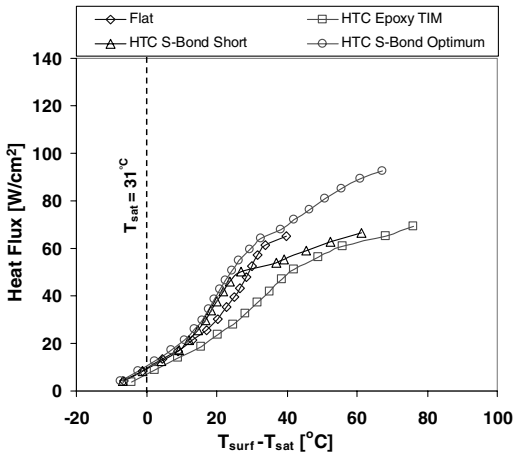

b) Liquid flow rate of 140 ml/min

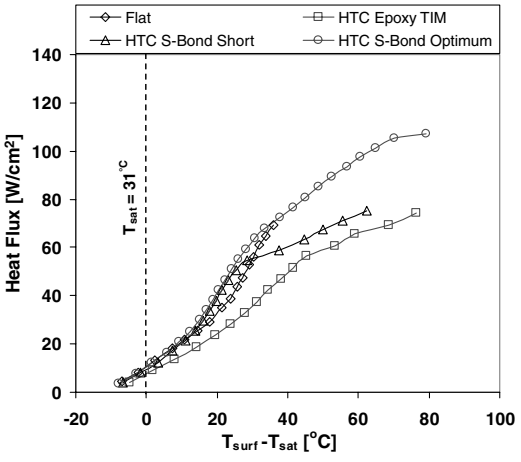

c) Liquid flow rate of 160 ml/min

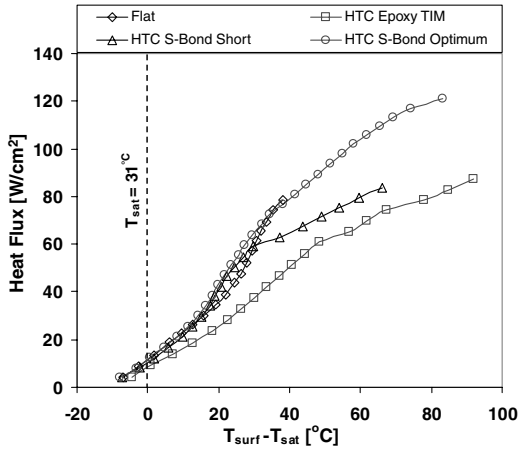

d) Liquid flow rate of 180 ml/min

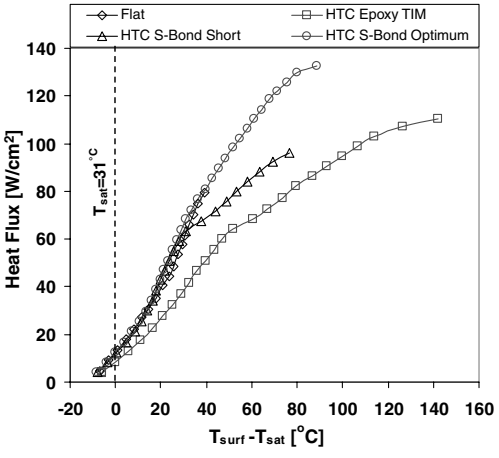

e) Liquid flow rate of 200 ml/min

Fig. 5 Heat flux as a function of superheat and volume flow rate: a) 120 ml/ min, b) 140 ml/ min, c) 160 ml/ min, d) 180 ml/ min, e) 200 ml/ min.

At each flow rate tested the CHF values achieved for the flat and HTC S-Bond short case were comparable (i.e., within 6 W/cm^2) with the exception of the 200 ml/ min flow rate. The superheat values at CHF for the HTC S-Bond short case tests exceeded that of the flat surface case by 28 $\leftrightarrow$ 37°C over the flow rate range tested. In the 120 and 140 ml/ min flow rate tests, the HTC epoxy TIM cases had the lowest heat flux performance for $\Delta T_{sup} > 11$°C. At flow rates ranging from 160 to 200 ml/ min, this trend in comparative heat flux performance held. However, the superheat values at which the separation of the heat flux curves began reduced to $\Delta T_{sup} \approx 5$°C. In each of the cases studied, the maximum observed heat flux occurred at a liquid flow rate of 200 ml/ min. For the flat, HTC epoxy TIM, HTC S-Bond short, and HTC S-Bond optimum cases, these values were 80, 110, 96, and 133 W/cm^2, respectively, (also shown in Table 3). However, for the flat case, the 180 ml/ min CHF value was 79 W/cm^2, indicating that flow rates greater than 180 ml/ min

Table 3 Summary of surface structure test data

Surface description	$\dot{V}$ volume flow rate, ml/ min	TIM	Nozzle height, mm	$\dot{q}''_{CHF}$, W/cm^2	CHF enhancement (relative to flat surface CHF), %	ΔT_{sup}, °C	$\eta_{2\text{-}\phi}$
Flat	120	——	17	56[a,c]	——	36.1	32.6
HTC epoxy TIM	120	Stycast 2850/Cat 11	17	63.3[b]	13.1	81.2	36.8
HTC S-Bond short	120	S-Bond	17	56.6[a]	1.1	64.9	32.9
HTC S-Bond optimum	120	S-Bond	22.9	79.9[a]	42.7	63.9	46.5
Flat	140	——	17	65[a,c]	——	40.0	34.4
HTC epoxy TIM	140	Stycast 2850/Cat 11	17	69.2[b]	6.4	76.2	36.6
HTC S-Bond short	140	S-Bond	17	66.6[a]	2.5	61.1	35.2
HTC S-Bond optimum	140	S-Bond	22.9	92.5[a]	42.3	67.2	48.9
Flat	160	——	17	69[a,c]	——	36.0	30.9
HTC epoxy TIM	160	Stycast 2850/Cat 11	17	74.4[b]	7.8	76.3	33.3
HTC S-Bond short	160	S-Bond	17	75.2[a]	9.0	62.5	33.6
HTC S-Bond optimum	160	S-Bond	22.9	107.3[a]	55.5	79.1	48.0
Flat	180	——	17	79[a,c]	——	38.0	30.6
HTC epoxy TIM	180	Stycast 2850/Cat 11	17	87.2[b]	10.4	92.0	33.8
HTC S-Bond short	180	S-Bond	17	83.4[a]	5.6	66.0	32.3
HTC S-Bond optimum	180	S-Bond	22.9	120.9[a]	53.0	83.1	46.9
Flat	200	——	17	80[a,c]	——	40.0	29.1
HTC epoxy TIM	200	Stycast 2850/Cat 11	17	110.3[a]	37.9	142.1	40.1
HTC S-Bond short	200	S-Bond	17	96.0[a]	20.0	76.5	34.9
HTC S-Bond optimum	200	S-Bond	22.9	132.5[a]	64.6	88.7	48.2

[a]CHF was attained
[b]Maximum heat flux taken at $T_{surf} \approx 115$°C
[c]Previously reported by Silk [28]

provide diminishing returns upon the flat surface heat flux. The 200 ml/ min HTC epoxy TIM case had the largest superheat observed ($\Delta T_{sup} \approx 143$°C at CHF) for all of the test cases.

IV. Effects of POCO HTC Foam Use

A. Flat Versus POCO HTC Foam Comparison

To determine the usefulness of POCO HTC foam as a heat transfer enhancement technique for spray cooling applications, heat flux performance must be examined relative to that of the flat surface case. Table 3 has a summary of the data for the flat and POCO HTC foam studies using both high-thermal-conductivity epoxy and S-Bond solder as the TIM. Included in the table is the volume flow rate onto the heater surface, the TIM used, the nozzle height relative to the copper surface, the CHF (or maximum heat flux attained), the maximum heat flux enhancement relative to the analogous flat surface test, the maximum superheat observed on the copper surface at the copper/foam interface, and the multiphase evaporation efficiency (defined in the nomenclature). As shown in Table 3, use of the POCO HTC foam provided a noticeable improvement in maximum heat flux performance (as well as multiphase evaporation efficiency) relative to that of the flat surface for all flow rates studied in the HTC S-Bond optimum case. However, for the HTC S-Bond short and HTC epoxy TIM cases, noticeable heat flux enhancement is not achieved for flow rates lower than 160 ml/ min. A review of Figs. 5a–5e show that heat flux performance for each of the flat surface volume flow rate studies exceeded that of the HTC epoxy TIM case at comparable superheat levels throughout their spray cooling curves (up to CHF). Heat flux performance for the flat surface flow rate studies only exceeded that for the HTC S-Bond short case at superheat levels ranging from 32°C up through the maximum superheat observed (i.e., CHF for the flat case). Superheat levels at which CHF occurred in both S-Bond TIM cases (shown in Figs. 5a–5e) exceeded those for the flat surface case at comparable volume flow rates by 20–40°C. The HTC epoxy TIM case tests attained heat fluxes greater than that of the flat surface tests only after reaching extensive superheat levels (i.e., $\Delta T_{sup} \geq 65$°C). In addition, heat flux variation as a function of volume flow rate was noticeable in the spray cooling curves for the flat surface cases throughout the single-phase and multiphase regimes, whereas, in the HTC epoxy TIM case, there was negligible heat flux variation for superheat levels below 40°C. As mentioned earlier, the HTC S-Bond optimum case achieved the highest heat flux performance for all cases at each of the flow rates studied. As such, the HTC S-Bond optimum case had the largest heat flux enhancement at CHF relative to that observed for the flat surface. Nonetheless, the heat flux enhancements observed in the HTC S-Bond optimum case (and the POCO HTC foam cases in general) was achieved at the sacrifice of elevated superheats at the copper/foam interface. The superheat levels attained at CHF for the HTC S-Bond optimum case exceeded those observed for the flat surface case by 20–48°C. For the 200 ml/ min flow rate test, the HTC S-Bond optimum case had an approximate copper surface temperature of 120°C at CHF. This temperature exceeds the range of commonly accepted servicing temperatures for the cooling of electronic components. Nonetheless, POCO HTC foam can be used as a high-heat-flux enhancement technique for alternate cooling applications that are not subject to failure or damage at moderate-to-high temperatures.

B. POCO HTC Foam Case Comparisons

Spray Optimization: As mentioned earlier, the HTC S-Bond optimum case had better heat flux performance than the flat surface. However, a comprehensive review of the studies performed (see Figs. 5a–5e) shows that this case also had better heat flux performance compared with the other POCO HTC foam cases investigated. This case also showed significant improvement in superheat levels observed at CHF relative to the HTC epoxy TIM case. The improved heat flux performance of the HTC S-Bond optimum case relative to the heat flux performance for the HTC S-Bond short case is a result of providing optimum spray coverage of the foam's top surface. A previous study by Mudawar and Estes [11] experimentally showed that optimization of the liquid spray coverage across the heater surface also results in optimum heat flux performance.

TIM Selection: As mentioned earlier (and shown in Figs. 5a–5e and Table 3), use of the POCO HTC foam provided an improvement in maximum heat flux performance (as well as multiphase efficiency) relative to the flat surface case at comparable volume flow rates for most of the test cases. Nonetheless, use of the foam also produced an increase in superheat levels for the copper surface at the copper/foam interface. Thus, one effect associated with the use of foam is increased superheating. Relative to the flat surface, use of the foam creates additional thermal resistances between the copper surface and the working fluid. The total thermal resistance for spray cooled enhanced surfaces using foam consists of thermal couplings between the bonding surface (copper in this case) and the foam (i.e., the thermal interface resistance), conductive resistance to heat flow

through the foam structure itself, and the convective resistance between the foam exterior and the working fluid. Each of these resistances may be considered a function of the foam's porosity. In the study by Shih et al. [19], the effective Nusselt number resulting from air flow through aluminum foam was experimentally determined as a function of foam porosity. The authors' study showed that the effective Nusselt number actually increased with decreasing foam porosity. In the study by Silk and Dick [27], the authors investigated the effective flow rate of PF-5060 liquid through a Poco Foam structure while spraying the top surface of the foam. The range of flow rates tested (120–200 ml/ min) were similar to those used in the present study. The authors determined that the liquid flow rate through the foam interior was not large enough to significantly affect the measured heat flux. Because the average pore size for the POCO HTC foam used in the present study is the same as that used by Silk and Dick [27] in their study and the present study's foam has a slightly lower density than that of the Poco Foam used in the study by Silk and Dick [27], convective flow through the POCO HTC foam interior is considered negligible. Thus, convective resistance to heat transfer through the interior of the foam is considered negligible in the present copper-to-working-fluid thermal resistance network. As such, convective resistance (and ultimately heat transfer) is limited to the exterior surfaces of the foam and porosity features only affect the heat flux in areas along the foam exterior that are in contact with the liquid. The determination that the foam heat transfer phenomena is limited to the respective foam's exterior surface is in agreement with the determinations of previous researchers such as Coursey et al. [22], Wong and Dybbs [30], and Jamin and Mohamad [20]. In the thermosyphon study by Coursey et al. [22], it was determined that the heat transfer that occurred was predominantly a surface phenomenon. Wong and Dybbs [30] experimentally showed that the temperature difference (i.e., the gradient) between the working fluid interior to a packed bed and the structure particles was approximately zero. Thus, the internal thermal resistance can be expected to be small as well. Furthermore, in the forced convection study (in which the working fluid was air) by Jamin and Mohamad [20], the authors concluded that the heat transfer between the foam and the working fluid was limited to the outer surface of the foam at the gas/foam interface.

Figure 6 shows thermal resistance (defined in the Nomenclature) at the maximum heat flux observed as a function of the volume flow rate for each of the study cases. Because thermal resistance is the inverse of thermal conductance, a lower thermal resistance allows heat to pass through a network of thermal couplings with lesser impedance and thereby lowers system temperatures at equilibrium. As shown in Fig. 6, the flat surface case has the lowest resistances throughout the flow rates tested. The second lowest is for that of the HTC S-Bond optimum case tests. The second highest set of resistances was observed for the HTC S-Bond short case tests. The largest resistances were observed for the HTC epoxy TIM case. The flat surface case had the lowest resistances because there was intimate contact between the working fluid and copper heater surface. This may be considered the best physical case. All the other cases had additional resistances inherent to their configuration, thereby increasing their total resistance.

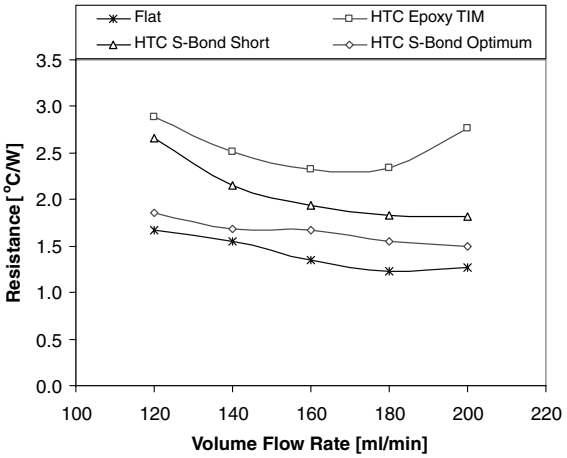

Fig. 6 Total thermal resistance between the copper surface and working fluid at a maximum heat flux tested as a function of volume flow rate.

Because the nozzle-to-foam distance used in the HTC epoxy TIM and HTC S-Bond short cases are the same, these studies are comparable. The decrease in resistance for the HTC epoxy TIM cases (shown in Fig. 6) at intermediate volume flow rates (i.e., 120–180 ml/ min) is due to the fact that these cases were not tested up through CHF, whereas the 200 ml/ min case was. The HTC S-Bond short case tests showed a noticeable decrease in resistance with increasing flow rate. There is also a decrease in thermal resistance relative to that for the HTC epoxy TIM case tests. The largest decrease (35% relative to the HTC epoxy TIM case) occurred at a flow rate of 200 ml/ min. Notwithstanding possible workmanship issues associated with the foam bonding process, resistances for the HTC epoxy TIM case tests may be considered strongly affected by the thermophysical properties of the bonding agent (i.e., epoxy versus solder).

The HTC S-Bond optimum case tests consistently had lower resistances compared with the HTC S-Bond short case tests. Because both have been bonded to their copper surfaces using the same technique (S-Bond soldering), the authors determined that the reduction in resistance is associated with the convective resistance at the foam/liquid interface. By optimizing the nozzle-to-foam distance, the convective resistance at the foam/liquid interface was reduced. The total reduction in resistance at the foam/liquid interface due to optimization of the liquid spray coverage across the top foam surface, as well as use of the S-Bond soldering technique to join the foam to the copper surface, helped approximate the experimentally determined thermal resistances to those of the flat surface throughout the range of volume flow rates tested. Relative to the worst case (i.e., the HTC epoxy TIM case), there was a 43% reduction in thermal resistance at the maximum volume flow rate of 200 ml/ min. Nonetheless, these resistances were still large enough to foster moderate superheating at the copper/foam interface (shown in Figs. 5a, 5d, and 5e) relative to the flat surface's performance.

C. Surface Roughness and Porosity

Although it was determined earlier that the POCO HTC foam's porosity had a negligible effect upon the heat flux within the foam's interior, pores located on the exterior at the liquid/foam interface may be considered surface enhancements (on the surface roughness scale) that promote enhanced heat transfer. Previous spray cooling studies [1] have shown that surface enhancements on the order of the surface roughness scale can promote heat flux enhancement when using a liquid atomizer for droplet breakup. However, the portion of the heat flux enhancement in the present POCO HTC foam studies that can be attributed to the effective surface roughness is unknown at this time.

V. Conclusions

Spray cooling heat flux measurements were performed for POCO HTC foam enhanced surfaces as well as a flat surface using PF-5060. Tests were performed under nominally degassed conditions (fluid at 41.4 kPa) for volume flow rates ranging from 120 to 200 ml/ min (a volumetric flux of 0.010–0.016 $m^3/m^2 \cdot s$). The nozzle height relative to the copper heater surface (17 mm) was held constant for the flat, HTC epoxy TIM, and the HTC S-Bond short study cases. However, the HTC S-Bond optimum case had a larger nozzle-to-foam distance ($\approx$23 mm) that provided optimum spray coverage of the foam impingement surface.

The flat surface's heat flux performance approximated to that of the HTC S-Bond optimum case with increasing flow rate. However, above a volume flow rate of 180 ml/ min, the flat surface showed diminishing returns upon the heat flux for increasing flow rates. The maximum CHF for the flat surface case was $\approx$80 W/cm^2. The POCO HTC foam surfaces each showed heat flux enhancement relative to the flat surface for each of the volume flow rates tested. Use

of the foam provided enhanced heat flux. However, it also created a thermal resistance to the heat flow path. This resulted in extensive superheating of the copper surface at the copper/foam interface. The foam study case with the least thermal resistance between the copper surface at the copper/foam interface and the working fluid was the HTC S-Bond optimum case. The maximum CHF for this study case was 133 W/cm^2 at a volume flow rate of 200 ml/ min with a superheat value of 89°C.

Acknowledgments

This research was supported by the Internal Research and Development Fund and the Thermal Engineering Branch at NASA Goddard Space Flight Center. Special thanks are given to Mario Martins, Richard Freburger, Jim Dye, and Alice Rector of NASA Goddard Space Flight Center for their test support, as well as Parker Hannifin's Gas Turbine Fluid Systems Division for supplying the spray nozzle.

References

[1] Sehmbey, M., Chow, L., Pais, M., and Mahefkey, T., "High Heat Flux Spray Cooling of Electronics," *12th Symposium on Space Nuclear Power and propulsion*, CP 324, American Institute of Physics, College Park, MD, Jan. 1995, pp. 903–909.

[2] Yang, J., Pais, M., and Chow, L., "Critical Heat Flux Limits in Secondary Gas Atomized Liquid Spray Cooling," *Experimental Heat Transfer*, Vol. 6, 1993, pp. 55–67.

[3] Estes, K. A., and Mudawar, I., "Correlation of Sauter Mean Diameter and Critical Heat Flux for Spray Cooling of Small Surfaces," *International Journal of Heat and Mass Transfer*, Vol. 38, No. 16, 1995, pp. 2985–2996. doi:10.1016/0017-9310(95)00046-C

[4] Yang, J., Chow, L., and Pais, M., "Nucleate Boiling Heat Transfer in Spray Cooling," *Journal of Heat Transfer*, Vol. 118, 1996, pp. 668–671. doi:10.1115/1.2822684

[5] Chen, R-H., Chow, L., and Navedo, J., "Effects of Spray Characteristics on Critical Heat Flux in Subcooled Water Spray Cooling," *International Journal of Heat and Mass Transfer*, Vol. 45, 2002, pp. 4033–4043. doi:10.1016/S0017-9310(02)00113-8

[6] Sehmbey, M., Pais, M., and Chow, L., "A Study of Diamond Laminated Surfaces in Evaporative Spray Cooling," *Thin Solid Films*, Vol. 212, 1992, pp. 25–29. doi:10.1016/0040-6090(92)90495-W

[7] Healy, W., Halvorson, P., Hartley, J., and Abdel-Khalik, S., "A Critical Heat Flux Correlation for Droplet Impact Cooling at Low Weber Numbers and Various Ambient Pressures," *International Journal of Heat and Mass Transfer*, Vol. 41, 1998, pp. 975–978. doi:10.1016/S0017-9310(97)00179-8

[8] Sawyer, M., Jeter, S., and Abdel-Khalik, S., "A Critical Heat Flux Correlation for Droplet Impact Cooling," *International Journal of Heat and Mass Transfer*, Vol. 40, No. 9, 1997, pp. 2123–2131. doi:10.1016/S0017-9310(96)00267-0

[9] Bernadin, J. D., and Mudawar, I., "The Leidenfrost Point: Experimental Study and Assessment of Existing Models," *Journal of Heat Transfer*, Vol. 121, 1999, pp. 894–903. doi:10.1115/1.2826080

[10] Pais, M., Chow, L., and Mahefkey, E., "Surface Roughness and its Effects on the Heat Transfer Mechanism of Spray Cooling," *Journal of Heat Transfer*, Vol. 114, No. 1, 1992, pp. 211–219. doi:10.1115/1.2911248

[11] Mudawar, I., and Estes, K., "Optimizing and Predicting CHF in Spray Cooling of a Square Surface," *Journal of Heat Transfer*, Vol. 118, 1996, pp. 672–679. doi:10.1115/1.2822685

[12] Qiao, Y. M., and Chandra, S., "Experiments on Adding a Surfactant to Water Drops Boiling on a Hot Surface," *Proceedings of the Royal Society of London*, Vol. 453, 1997, pp. 673–689. doi:10.1098/rspa.1997.0038

[13] Qiao, Y., and Chandra, S., "Spray Cooling Enhancement by Addition of a Surfactant," *Journal of Heat Transfer*, Vol. 120, 1998, pp. 92–98. doi:10.1115/1.2830070

[14] Mesler, R., "Surface Roughness and Its Effects on the Heat Transfer Mechanism of Spray Cooling," *Journal of Heat Transfer*, Vol. 115, 1993, pp. 1083–1085. doi:10.1115/1.2911372

[15] Rini, D., Chen, R.-H., Chow, L., "Bubble Behavior and Nucleate Boiling Heat Transfer in Saturated FC-72 Spray Cooling," *Journal of Heat Transfer*, Vol. 124, 2002, pp. 63–72. doi:10.1115/1.1418365

[16] Hsieh, C., and Yao, S., "Evaporative Heat Transfer Characteristics of a Water Spray on Micro-Structured Silicon Surfaces," *International Journal of Heat and Mass Transfer*, Vol. 49, 2006, pp. 962–974. doi:10.1016/j.ijheatmasstransfer.2005.09.013

[17] Silk, E. A., Kim, J., and Kiger, K., "Spray Cooling of Enhanced Surfaces: Impact of Structured Surface Geometry and Spray Axis Inclination," *International Journal of Heat and Mass Transfer*, Vol. 49, No. 25/26, 2006, pp. 4910–4920. doi:10.1016/j.ijheatmasstransfer.2006.05.031

[18] Coursey, J., Kim, J., and Kiger, K., "Spray Cooling of High Aspect Ratio Open Microchannels," *Journal of Heat Transfer*, Vol. 129, No. 8, 2007, pp. 1052–1059. doi:10.1115/1.2737476

[19] Shih, W. H., Chiu, W. C., and Hsieh, W. H., "Height Effect on Heat-Transfer Characteristics of Aluminum Foam Heat Sinks," *Journal of Heat Transfer*, Vol. 128, 2006, pp. 530–537. doi:10.1115/1.2188461

[20] Jamin, Y. L., and Mohamad, A. A., "Enhanced Heat Transfer Using Porous Carbon Foam in Cross Flow-Part I: Forced Convection," *Journal of Heat Transfer*, Vol. 129, 2007, pp. 735–742. doi:10.1115/1.2717240

[21] Salas, K., and Waas, A., "Convective Heat Transfer in Open Cell Metal Foams," *Journal of Heat Transfer*, Vol. 129, 2007, pp. 1217–1229. doi:10.1115/1.2739598

[22] Coursey, J. S., Kim, J., and Boudreaux, P. J., "Performance of Graphite Foam Evaporator for Use in Thermal Management," *Journal of Electronic Packaging*, Vol. 127, 2005, pp. 127–134. doi:10.1115/1.1871193

[23] Kim, J. H., Rainey, K. N., You, S. M., and Pak, J. Y., "Mechanism of Nucleate Boiling Heat Transfer Enhancement From Microporous Surfaces in Saturated FC-72," *Journal of Heat Transfer*, Vol. 124, 2002, pp. 500–506. doi:10.1115/1.1469548

[24] Parker, J. L., and El-Genk, M. S., "Effect of Surface Orientation on Nucleate Boiling of FC-72 on Porous Graphite," *Journal of Heat Transfer*, Vol. 128, 2006, pp. 1159–1175. doi:10.1115/1.2352783

[25] Li, C., and Peterson, G. P., "Experimental Studies on CHF of Pool Boiling on Horizontal Conductive Micro Porous Coated Surfaces," *Space Technology and Applications International Forum*, Feb. 2008, Albuquerque, NM., AIP Conference Proceedings, 2008, pp. 12–20.

[26] Pauken, M., Emis, N., and Watkins, B., "Thermal Energy Storage Technology Developments," *Space Technology and Applications International Forum*, American Institute of Physics, College Park, MD, Feb. 2007, pp. 412–420.

[27] Silk, E. A., and Dick, D. O., "Foam Spray Cooling Heat Transfer Study," *19th International Symposium on Transport Phenomena*, Univ. of Iceland Paper 176, Aug. 2008.

[28] Silk, E. A., "Investigation of Pore Size Effect on Spray Cooling Heat Transfer With Porous Tunnels," *Space Technology and Applications International Forum*, American Institute of Physics, College Park, MD, Feb. 2008, pp. 112–122.

[29] Arnold, W., Hartman, T., and McQuillen, J., "Chemical Characterization and Thermal Stressing Studies of Perfluorohexane Fluids for Space-Based Applications," *Journal of Spacecraft and Rockets*, Vol. 44, No. 1, 2007, pp. 94–101. doi:10.2514/1.22537

[30] Wong, K. F., and Dybbs, A., "An Experimental Study of Thermal Equilibrium in Liquid Saturated Porous Media," *International Journal of Heat and Mass Transfer*, Vol. 19, 1976, pp. 234–235. doi:10.1016/0017-9310(76)90120-4